Volume 7 | Number 24 | 21 December 2015 | Pages 10069–10458

Analytical Methods

www.rsc.org/methods

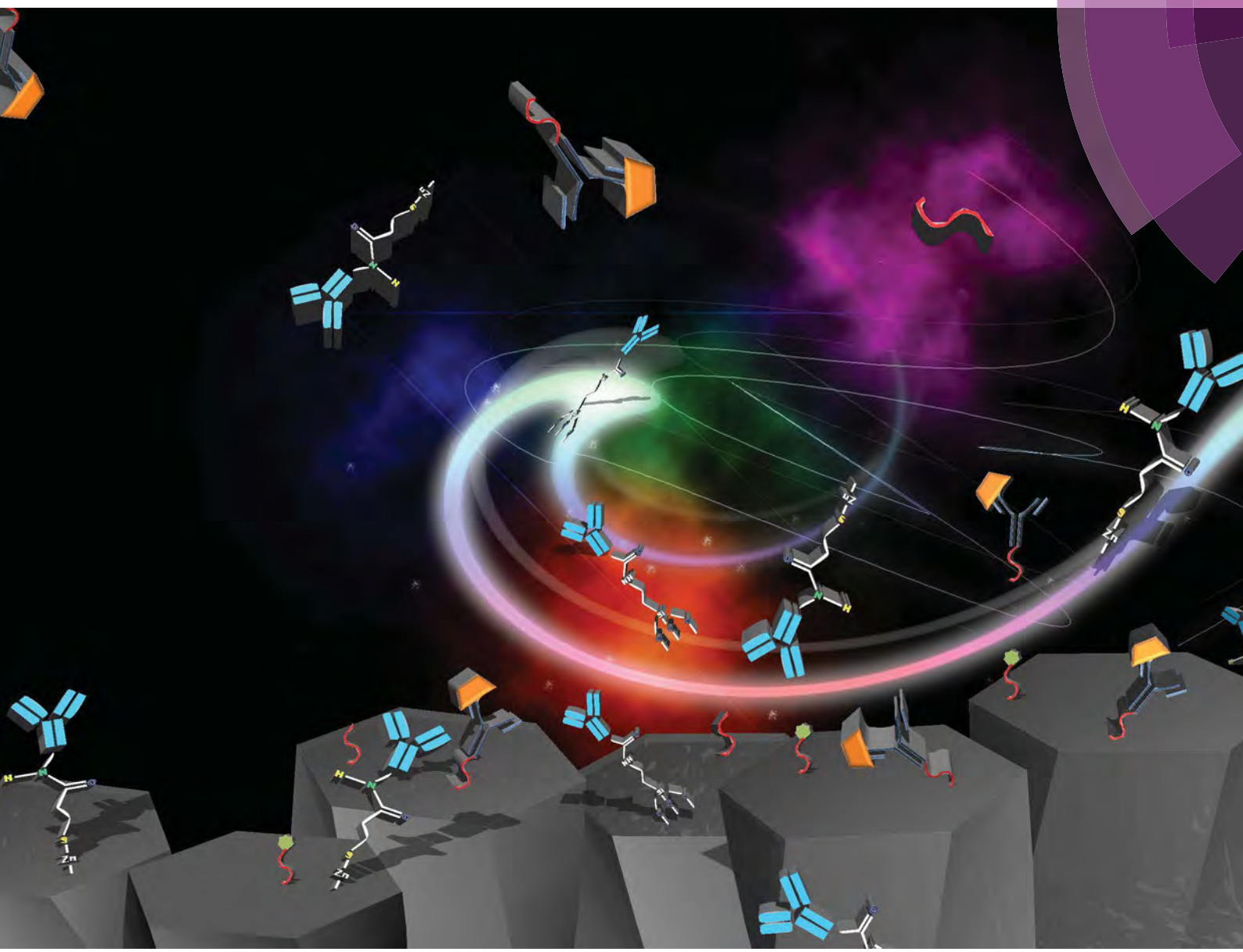

ISSN 1759-9660

ROYAL SOCIETY OF CHEMISTRY

PAPER

Shalini Prasad *et al.*

A novel approach for electrical tuning of nano-textured zinc oxide surfaces for ultra-sensitive troponin-T detection

Analytical Methods

PAPER

View Article Online
View Journal | View Issue

Cite this: *Anal. Methods*, 2015, **7**, 10136

A novel approach for electrical tuning of nano-textured zinc oxide surfaces for ultra-sensitive troponin-T detection

Rujuta D. Munje,[a] Michael Jacobs,[a] Sriram Muthukumar,[b] Bilal Quadri,[a] Nandhinee Radha Shanmugam[a] and Shalini Prasad*[a]

Received 4th August 2015
Accepted 6th August 2015

DOI: 10.1039/c5ay02052b

www.rsc.org/methods

We have developed a label-free, non-faradaic, electrochemical sensor for ultra-sensitive detection of a cardiac biomarker, troponin-T by utilizing the stoichiometric surface compositions of nanotextured zinc oxide (ZnO) thin films. In this study, we show how the performance of a nanotextured zinc oxide based non-faradaic biosensor is modulated by differences in the fabrication parameters of the metal oxide thin film as well as the choice of cross-linkers. Two cross-linking molecules, dithiobis succinimidyl propionate and 3-aminopropyl triethoxysilane, demonstrate significantly different binding chemistries with zinc oxide. The non-faradaic electrochemical behaviour of the sensor due to the two linkers is compared by analyzing the troponin-T dose response using electrochemical impedance spectroscopy (EIS). The sensor performance associated with both linkers is compared based on the dynamic range and limit of detection. The sensor utilizing zinc surface terminations demonstrated a wider dynamic range between the two linkers. This range extended from 26% to 54% in phosphate buffered saline and from 21% to 65% in human serum, for a concentration range from 10 fg mL^{-1} to 1 ng mL^{-1} of troponin-T. The limit of detection was found to be at 10 fg mL^{-1} and has potential utility in the development of point-of-care (POC) diagnostics for cardiovascular diseases. Fluorescence quantification analysis was also performed to further validate the specificity of the linker binding to the ZnO films. An ultrasensitive troponin-T biosensor can be designed by leveraging the zinc termination based surface chemistry for selective protein immobilization.

1. Introduction

Approximately 1.5 million cases of acute myocardial infarction (AMI) occur each year in the United States alone. Rapid and suitable treatment for AMI is possible if patients are diagnosed reliably in an early stage. Usually, this diagnosis is done using electrocardiographs that reduce the delay in treatment. However, coupling this technology with biomarker based diagnostics may enable robust diagnostics of AMI patients. It has been proved that cardiac-specific contractile proteins such as troponin have great potential for successful prediction of AMI. Troponin-T has enhanced specificity and efficacy, has higher diagnostic efficiency as compared to other cardiac biomarkers and persists longer in circulation.[1] Cardiac troponin-T is a structural protein that is released into the bloodstream when damage to cardiac muscle occurs and is proportional to the intensity of damage. Its level remains elevated from 3.5 hours upto 10 days after the onset of stroke.[2] The normal serum troponin-T level is <0.01 ng mL^{-1}. After a stroke, the serum troponin-T level can elevate upto 0.266 ng mL^{-1} or even higher.[3] Quantitative point-of-care troponin-T assays are now available but most of them use optical transduction mechanisms, including electrochemiluminescence, which are not suitable for point-of-care diagnostics. Also, these techniques typically use labels or tags that modify the biomolecule conformation and increase the noise in measurement.

Electrochemical sensors are being widely used in the field of industry, medicine, and agriculture for their robustness as a sensitive, cost-effective, and rapid form of molecular detection.[4] Electrochemical detection of troponin-T reported previously had used carbon nanotubes supported by polyethyleneimine films and demonstrated a limit of detection (LOD) of 0.033 ng mL^{-1}.[5] Another study had demonstrated use of a streptavidin polystyrene microsphere modified screen-printed electrode surface in order to achieve the LOD of 0.2 ng mL^{-1} of troponin T.[6] Additionally, another study had demonstrated templated electropolymerization of aminophenol (AP) in the presence of protein and achieved a LOD of 1.5 μg mL^{-1}.[7] While these faradaic strategies have shown the sensitivity for POC clinical diagnostics, they present the challenge of modifying the molecule under test, which is a significant problem in designing

[a]*Department of Bioengineering, University of Texas at Dallas, 800 W. Campbell Road, EC 39, Richardson, TX 75080, USA*

[b]*Enlisense LLC, 1813 Audubon Pond Way, Allen, TX 75013, USA. E-mail: shalini.prasad@utdallas.edu*

protein immunosensor assays.[4] Hence, the use of non-faradaic electrochemical transduction strategies for protein biomolecule detection and quantification has been demonstrated in this study. While non-faradaic techniques have been shown to be highly sensitive, there have been challenges in achieving selectivity. In this paper, we address the challenge of achieving selectivity in non-faradaic ZnO thin film biosensors for protein detection by using cardiac troponin-T as the study protein through the utilization of stoichiometric distribution of surface terminations.

The surface and bulk properties of zinc oxide (ZnO) have for years made it an appealing material for industrial purposes such as gas-sensing, absorption[8] and bio-sensing.[9–12] ZnO exhibits properties like wide bandgap, strong luminescence, high piezoelectric constant and biocompatibility.[13] The focus of this paper is investigating the use of ZnO for designing diagnostic protein biosensors, which will enable clinical point-of-care (POC) applications. One of the useful properties of ZnO is the ability to tune its electrical characteristics and surface states based on deposition.[14] The lattice structure of ZnO exhibits a tetrahedral arrangement through the alternate stacking of Zn^{2+} and O^{2-} ions. Due to the nature of its growth mechanism, each columnar ZnO structure terminates with either a polar zinc or oxygen surface.[15] These surface characteristics of ZnO films can therefore be leveraged for bio-sensing.[16] Tailoring the terminations on the polar ZnO surface would enhance the capacity of the film for performing the desired biochemical function, improving the sensor selectivity.

In this paper, we analysed the ZnO sputter deposited films with and without oxygen flow. The linker with a thiol group, dithiobis(succinimidyl-propionate) (DSP) that has specificity in binding to the zinc terminated sites was functionalized on ZnO thin films deposited without oxygen flow, while the linker with the presence of silane group, 3-aminopropyl triethoxysilane (APTES) that has specificity in binding to the oxygen terminated sites was functionalized on ZnO thin films deposited with oxygen flow. We have specifically focused on analyzing the methods of selective functionalization of surface terminations and investigating the biosensor performance for troponin-T detection from phosphate buffered saline (PBS). We have then tested human serum (HS) samples containing variable doses of antigen to demonstrate the potential of the sensor for clinical POC diagnostics. Quantification of each linker molecule bound to the ZnO surface and its utility in biosensor performance was evaluated by using non-faradaic EIS. This is supported through fluorescence analysis using fluorophores.

2. Materials and methods

2.1 ZnO deposition and substrate preparation

EIS studies were performed using a Gamry Reference 600 potentiostat on FR-4 printed circuit board (PCB) substrates with electroplated gold electrodes shown in Fig. 1(a). The gold electrodes measured 1 mm in width and are designed in an interdigitated, concentric circular fashion with 1 mm spacing between each. The diameter of the outer concentric circle measures 13 mm. The entire portion of gold electrodes was covered with ZnO deposition. Fig. 1(b) shows the assembled sensor with polydimethylsiloxane (PDMS) manifold used for EIS testing. Fig. 1(c) provides a visualization of the columnar nanotexturing of the ZnO film through SEM images taken using a Zeiss SUPRA-40 scanning electron microscope. The substrates used for fluorescence experiments were 25 × 75 mm microscope slides (Thermo Fisher Scientific Inc. – Waltham, MA).

ZnO thin films were sputtered onto each substrate using an AJA Orion RF magnetron with a 99.999% ZnO target (Kurt J. Lesker) for 30 minutes at 140 watt power. For the deposition of No–O_2 films 12 standard cubic centimeters per minute (sccm) flow of argon was used and for the deposition of With-O_2 films a 2 sccm 100% O_2 and 10 sccm argon flow rate was used in the sputter chamber. The thickness of the film deposited during each run was measured with a Veeco Dektak 8 profilometer and was ~90–100 nm. The resistivity was measured using the Alessi CPS-7089-17 4-point probe and was around 34.3–64.5 Ω.cm on silicon substrates.

2.2 Linker functionalization

DSP is a homobifunctional cross-linking molecule consisting of two *N*-hydroxysuccinimide (NHS) groups attached to a spacer arm held together by a disulfide bond as shown in Fig. 1(d). NHS esters react with primary amines in proteins to form stable amide bonds. A 50 mmol DSP (Thermo Fisher Scientific Inc. – Waltham, MA) was diluted in dimethylsulfoxide (DMSO) (Thermo Fisher Scientific Inc. – Waltham, MA) and incubated for 30 minutes. Thiol groups have an affinity for positively charged zinc ions based on formation of stable zinc–sulphur bonds. Hence, this type of thiol linker molecule preferentially binds to the zinc terminated surfaces on the ZnO film.[16] Three washes with 1× DMSO were then performed to remove any unbound DSP.

APTES (3-aminopropyl triethoxysilane), as shown in Fig. 1(e), is an aminosilane molecule that silanizes by reacting with the hydroxyl groups on the oxide surfaces. The oxygen terminated ends of ZnO after forming hydroxyl groups allow for condensation reactions to occur between the APTES molecules and the ZnO surface.[17] Firstly, the substrates were sonicated in a solution containing APTES (Thermo Fisher Scientific Inc. – Waltham, MA) in ethanol 2% volume/volume for 1.5 minutes. These substrates were then dip coated in solution for 15 minutes. After sonication in ethanol for 2 minutes, 10 minute baking at 100 °C in an enclosed nitrogen gas chamber was carried out. The substrates are baked in an inert environment to avoid silanization of APTES due to environmental oxygen.

2.3 Immunoassay for non-faradaic EIS study and troponin-T detection

After 50 mmol DSP linker was incubated on PCB substrates, they were incubated with a monoclonal antibody to troponin-T (Abcam – Cambridge, MA) at 1 μg mL^{-1} in PBS (Thermo Fisher Scientific Inc. – Waltham, MA). It was incubated for 30 minutes at room temperature followed by three PBS washes. The antibody concentration used and its incubation time were optimized for the current sensor configuration in our previous

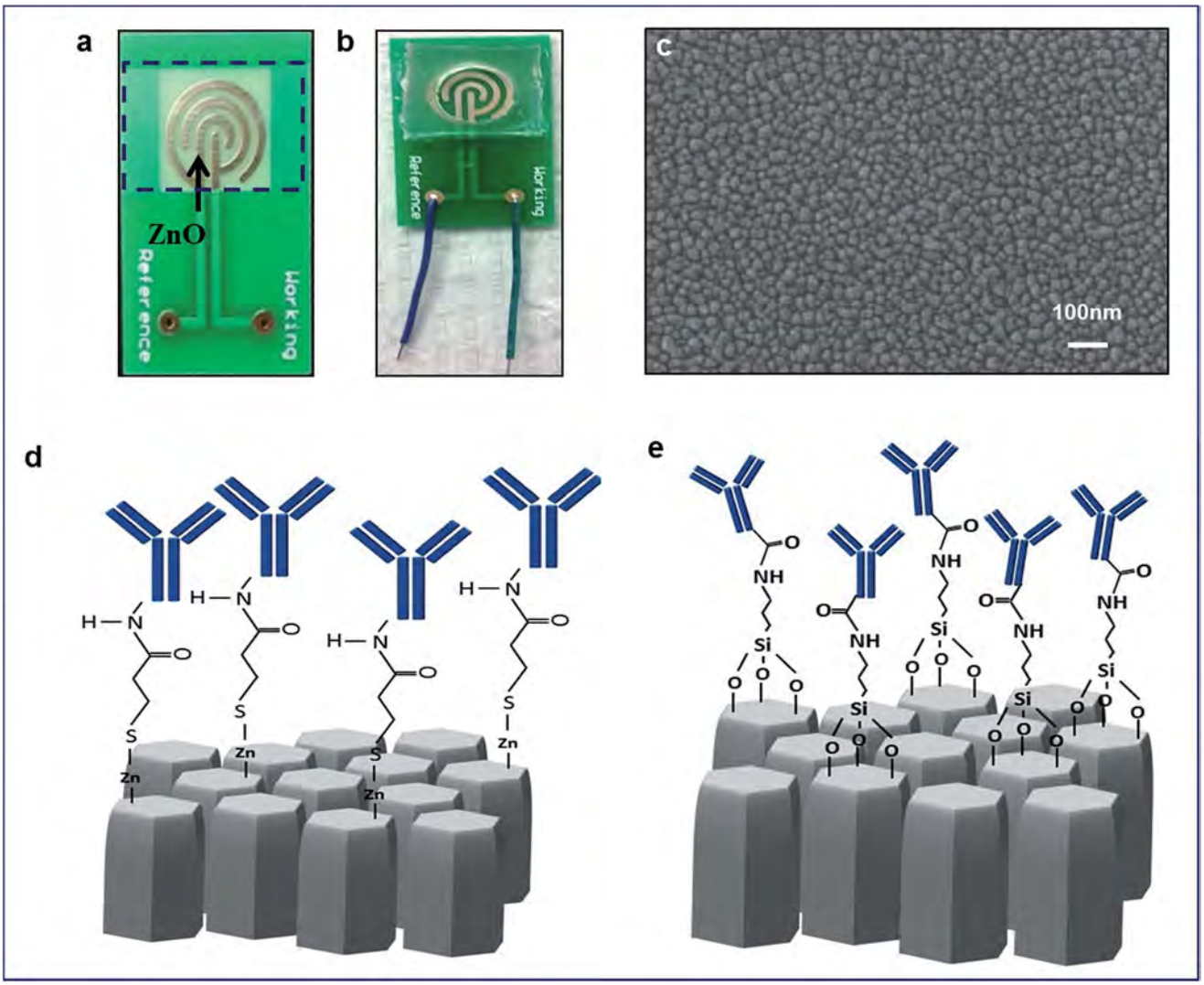

Fig. 1 (a) Sensor with sputtered ZnO over a gold electrode pattern; (b) assembled sensor for bio-sensing using EIS; (c) SEM of a nano-textured ZnO thin film; (d) immunoassay setup on the ZnO surface using DSP bound with troponin-T antibody; and (e) immunoassay setup on the ZnO surface using APTES bound with a troponin-T antibody.

study.[18] Next, 200 μL of Superblock (Thermo Fisher Scientific Inc. – Waltham, MA) was dispensed onto the sensor for 15 minutes to block any unbound linker sites. This was followed by three PBS washes and the measurement was obtained for the last wash. This reading corresponds to the baseline or zero-concentration value for the experiment with which antigen-containing samples were compared. For experiments with HS, this wash was carried out with HS in order to determine the baseline. Troponin-T (US Biological – Salem, MA) was diluted in PBS and in HS (Thermo Fisher Scientific Inc. – Waltham, MA) from 10 fg mL^{-1} to 1 ng mL^{-1}. Each solution was added from lower to higher concentration to the sensor and allowed to incubate for 20 minutes before the impedance measurement was taken.

When using the APTES linker, a 100 μL solution of 20 mmol 1-ethyl-3-(3-dimethylaminopropyl) carbodiimide (EDC) (Thermo Fisher Scientific Inc. – Waltham, MA) and 50 mmol *N*-hydroxysuccinimide (NHS) (Thermo Fisher Scientific Inc. – Waltham, MA) solution in PBS was prepared. Following the 15 minute incubation of the APTES coating on a ZnO sputtered PCB substrate, the EDC–NHS mixture was dispensed on the chips and incubated for 30 minutes. This was followed by a 1 h incubation of a 1 μg mL^{-1} antibody to a troponin-T solution in PBS on the substrate. The EDC–NHS will first bind to carboxylic groups of the antibody and the NHS-ester of EDC–NHS would bind to amine of APTES on the substrate. The EDC–NHS solution modulates the carboxyl groups of the antibody with an NHS group at the base of the heavy chain in the Fc region. This then allows for conjugation with the available amine group on the APTES molecules. This similar functionalization has been used by various other studies for the purpose of building a bio-immunoassay.[19–21] From this point, the remainder of the immunoassay preparation and troponin-T detection steps was identical to those performed with the DSP linker.

2.4 Fluorophore study

The qualitative analysis of binding of two types of linkers to the ZnO surface was done by attaching a Rhodamine 123 (Sigma-Aldrich – St. Louis, MO) molecule to the cross-linkers. This fluorophore molecule binds to the NHS end. 75 μL of 50 mmol DSP linker was incubated on ZnO sputtered glass substrates for 30 minutes. For the APTES linker, glass substrates were functionalized for 15 minutes as stated in Section 2.2. The EDC–NHS solution was incubated for 30 minutes. Afterwards, for both linkers, 75 μL of 2 mmol Rhodamine 123 solution was injected onto the substrates and incubated for 1 hour. Fluorescence was characterized by capturing images using a Zeiss Axio Observer microscope with excitation at 480 nm and emission at 536 nm, specific to Rhodamine 123 molecules. The substrates were exposed to excitation for around 50 μs. In total 15 images were captured for each sample and 3 such samples were studied for each linker. Every image was further processed using the MATLAB image processing toolbox (Mathworks – Natick, MA) to find out the quantity of fluorescent pixels corresponding to the binding of Rhodamine 123 to the linker.

3. Results and discussion

3.1 Troponin-T detection using EIS

As summarized in the review by Randviir and Banks,[4] EIS can be used towards the development of biocompatible surface chemistries for impedimetric immunosensing of biological samples. This work utilizes EIS for electrical quantification and analysis of linker driven biosensor performance over a range of frequencies from 0.1 Hz to 10 KHz. Nyquist plots of the troponin-T antigen aliquoted in PBS and immobilized at the electrode surface functionalized using DSP on No–O_2 ZnO thin films are depicted in Fig. 2(a). On similar lines, Fig. 2(b) represents Nyquist plots of the APTES linker on With-O_2 ZnO thin films. Sensor measurements for both linkers were conducted with $n = 3$ replicates. It is to be noted that troponin-T concentrations ranging from 10 fg mL^{-1} to 1 ng mL^{-1} were

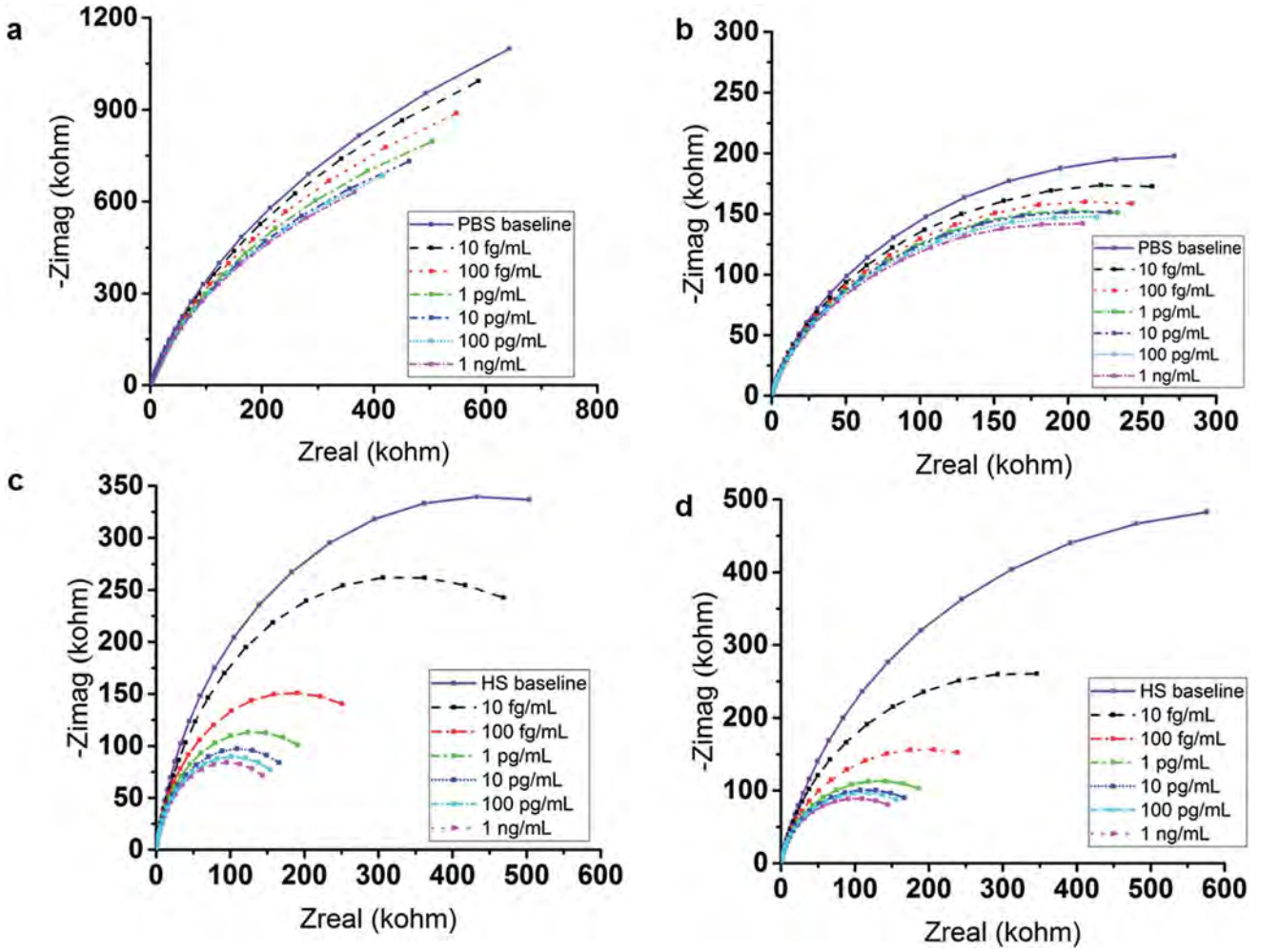

Fig. 2 Non-faradaic impedance spectra (Nyquist plots) for baseline and 10 fg mL^{-1} to 1 ng mL^{-1} troponin-T concentrations: (a) troponin-T diluted in PBS and binding to an antibody functionalized using a DSP linker; (b) troponin-T diluted in PBS and binding to an antibody functionalized using an APTES linker; (c) troponin-T diluted in HS and binding to antibody functionalized using a DSP linker; and (d) troponin-T diluted in HS and binding to an antibody functionalized using an APTES linker.

tested for both linkers. The entire analysis is repeated for the troponin-T antigen diluted in HS with $n = 2$ replicates with the rest of the experimental parameters remaining the same. Nyquist plots for these experiments using DSP and APTES linkers are demonstrated in Fig. 2(c) and (d) respectively.

The shape of the Nyquist plots in all cases consists of a large semicircle region that is not accompanied by a straight line. The absence of a redox label produces only non-faradaic impedances. Thus the parameters quantifying the electron transfer in the equivalent circuit representation of the sensor system, such as R_{ct} and Warburg impedance, become infinite.[22] This explains the shape of the Nyquist plots obtained across all experiments.

Furthermore, as the parameters R_{ct} and Warburg impedance are infinite, they can be ignored in the sensor equivalent circuit representation. With these parameters ignored, the imaginary part of the equivalent circuit impedance *i.e.* Z_{imag} is inversely proportional to the capacitance of the electrical double layer (EDL), at a particular frequency. This EDL can be perturbed due to binding of antibodies and troponin-T antigen at the electrode surface. It can be observed from the graphs that in all the cases, the range of Z_{imag} decreases as the concentration of troponin-T is increased. This can be attributed to the changes in capacitance of the EDL. The electrically charged troponin-T molecules alter the dielectric permittivity of the EDL thereby affecting the capacitance.[22] Thus in this case, the impedance decrease might have originated from the increase in the amount of hydrated proteins.[22]

In addition to its impact on Z_{imag}, the presence of higher surface concentration of troponin-T is also observed to lead to reduction in the value of Z_{real}. This observation can be potentially related to changes in the conductivity of solution gradient within the EDL due to accumulation of biomolecules. The observations associated with Z_{imag} and Z_{real} are applicable to both PBS and HS. Additionally, in the case of dilutions in HS, an extremely slow electron transfer is observed.[22] This might be due to some species present in human serum undergoing electrochemical conversion, contributing to the slight charge transfer.

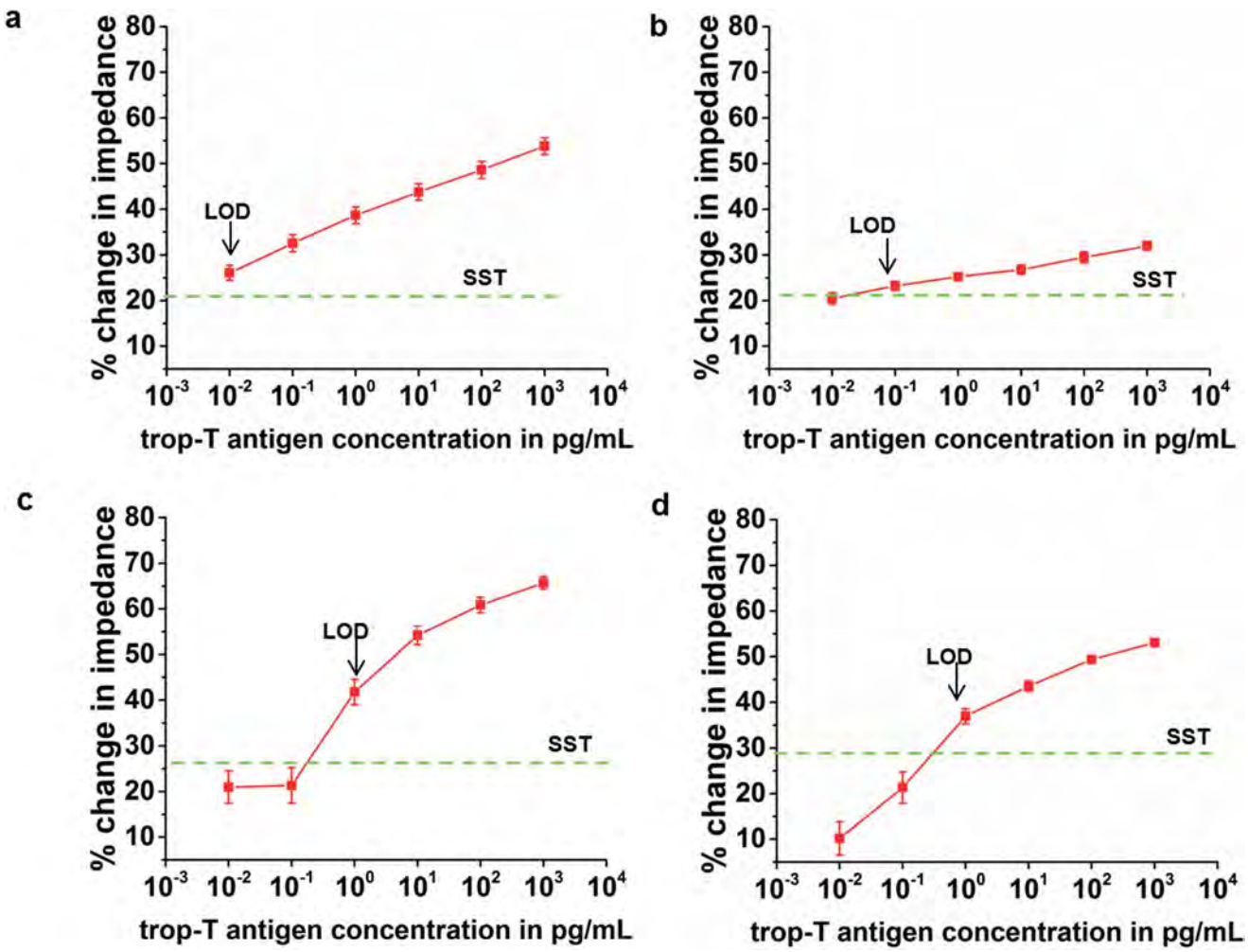

Fig. 3 Dose–response curves in terms of percent change in total impedance Z_{mod} upon sensing troponin-T concentrations from 10 fg mL^{-1} to 1 ng mL^{-1}: (a) troponin-T diluted in PBS and binding to an antibody functionalized using a DSP linker; (b) troponin-T diluted in PBS and binding to an antibody functionalized using an APTES linker; (c) troponin-T diluted in HS and binding to an antibody functionalized using a DSP linker; and (d) troponin-T diluted in HS and binding to an antibody functionalized using an APTES linker.

The difference in the surface chemistries of DSP based immunoassay and APTES based immunoassay can be interpreted from the shape of Nyquist plots. The Nyquist plots shown in Fig. 2(a) and 3(a) of the DSP based linker demonstrate a higher capacitive effect than resistive effect as the semicircle curve is not dropping at lower frequencies, indicating the phase angle to be higher than 50°. Whereas, under similar analysis for the APTES based immunoassay, it can be noticed from Nyquist plots that the semicircle has dropped at lower frequencies below 0.5 Hz with the phase angle approaching 30°, indicating more resistive behaviour than capacitive behaviour. This performance is hypothesized due to the formation of a monolayer on the ZnO surface in the case of an APTES linker, but not present in the case of a DSP linker.

In the next part of analysis, baseline impedance measurement was used as a reference for comparison of change in impedance values for a range of antigen concentrations binding to the immobilized troponin-T antibody. The dose–response curves are demonstrated in Fig. 3, where the impedance change is plotted as a function of troponin-T concentration over a 10 fg mL^{-1} to 1 ng mL^{-1} range by using the following eqn (1),

$$\% \text{ Change in total impedance} = \left(\frac{\left(Z_{\text{baseline(mod)}} - Z_{\text{mod}}\right)}{Z_{\text{baseline(mod)}}}\right) \times 100 \quad (1)$$

It is to be noted that the quantitative analysis presented in Fig. 3 is performed using impedance at the frequency for which maximum signal-to-noise ratio is obtained (~100 Hz). Furthermore, Z_{mod} (*i.e.* total impedance) values were used for representing the dose–response curves as these also include resistive noise due to a complex fluid medium such as human serum.

For samples spiked in PBS from 10 fg mL^{-1} to 1 ng mL^{-1} and dispensed over a DSP functionalized linker, the change in impedance varies with the dynamic range of 26% to 54% as shown in Fig. 3(a). For the APTES linker, it changes from 20% to 32% as shown in Fig. 3(b). This indicates higher changes in electrical double layer impedance due to DSP and zinc termination interaction. We observed a linear correlation between percent change in impedance and logarithmically increasing surface concentration. Furthermore, the linear fit of the dose–response curves in the case of DSP based immunoassay had R^2 values of 0.9958 and 0.992 for the APTES based immunoassay. This linear correlation is hypothesized to be due to rise of Donnan potential, which depends logarithmically on the concentration of immobilized biomolecules.[23]

For samples spiked in HS, as demonstrated in Fig. 3(c), the DSP linker based immunoassay shows impedance changes in the dynamic range of 21% to 65% for varying antigen concentrations. For the APTES linker based immunoassay, as shown in Fig. 3(d), the range reduced to 11% to 52%. The linearity coefficient of the dose–response curve decreases for both DSP (0.923) and for APTES (0.883) in the case of human serum as compared to the PBS buffer medium. It is hypothesized to be due to the complex nature of the human serum medium, where the resistive contribution due to interferents affected the total measured impedance.

Limit of detection (LOD) is identified as the lowest troponin-T concentration likely to be reliably distinguished from the limit of blank and at which detection is feasible.[24] The limit of blank is estimated by measuring replicates of a blank buffer sample and calculating the mean result and standard deviation.[24] A signal to noise ratio of 3 was identified as the robust indicator of sensor performance and the specific signal threshold (SST) impedance as three times the noise signal is calculated. The noise level is defined as the difference in the reading between average antibody measurement and average baseline (zero dose) measurement.[25] The limits of detection in a PBS medium for DSP and APTES linkers were found to be 10 fg mL^{-1} and 100 fg mL^{-1} respectively. Comparing both the dynamic range and limit of detection in PBS, DSP functionalized surfaces perform better than APTES functionalized surfaces. However, in the case of HS, the limit of detection was observed to be 1 pg mL^{-1} for both DSP and APTES linkers. The dynamic range in HS was higher for DSP linker functionalized surfaces. Also, while using an APTES linker in a HS medium, the sensor saturates at 1 ng mL^{-1}. The wider dynamic range with the DSP linker is advantageous when the sensor can be calibrated to obtain distinguishable higher percent change for the small changes in the concentrations of troponin-T to be detected. But at the same time lower limit of detection (LOD) needs to be achieved for ultra-sensitivity. Overall, it is evident that in both PBS and HS, the DSP linker binding to the ZnO surface is capable of achieving enhanced performance with greater precision as compared to APTES.

The LODs of 10 fg mL^{-1} and 1 pg mL^{-1} obtained using a DSP linker in PBS and HS respectively are lower than the commercial standards available currently in the market. Also the total diagnosis time for our biosensor was 15 minutes for a particular antigen concentration. A Cobas h 232 POC system available commercially has an LOD of 50 ng mL^{-1} and takes 8–12 minutes for detection. Also, Elecsys TnT-hs, a laboratory based test by Roche, has a LOD of 5 ng mL^{-1} and takes 18 minutes. A Cobas e 411 analyzer for troponin-T has a LOD of 10 ng mL^{-1} and specifies 3–10 minutes as test duration time. All these products are based on the electrochemiluminescence assay. Thus the developed biosensor shows improved sensitivity and comparable time of detection over the commercially available market standards.

3.2 Fluorescence analysis

We performed fluorescence studies to validate the binding specificity of DSP and APTES linkers to the ZnO surface through qualitative confirmation. These experiments provide visual confirmation of biomolecule binding. The linker molecules were modified with the fluorescent marker Rhodamine 123 for this study, which has the capability to bind to the same functional groups as the antibody in the immunoassay experiments. Fig. 4(a) displays the relative effectiveness of the binding of DSP and APTES linkers in terms of percentage of fluorescent pixel intensity. Higher fluorescent pixel intensity due to higher

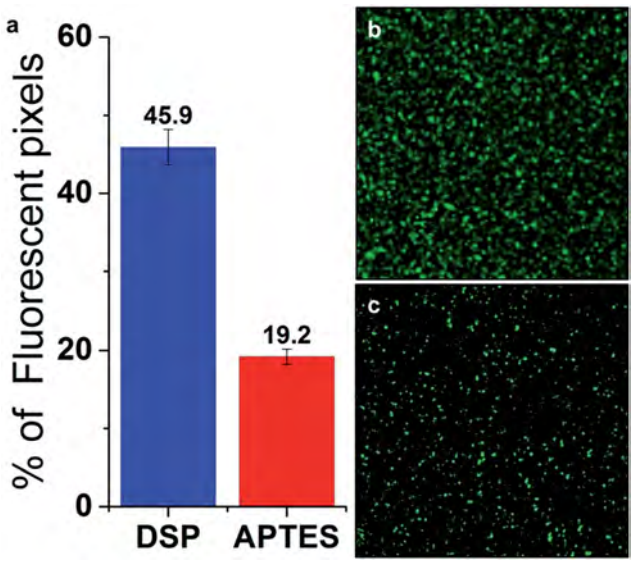

Fig. 4 (a) Fluorescent pixel comparison of DSP and APTES; (b) Rhodamine 123 functionalized using a DSP linker on a ZnO nano-textured surface sputtered without O_2; and (c) Rhodamine 123 functionalized using an APTES linker on a ZnO nano-textured surface sputtered with O_2.

binding of Rhodamine 123 can be interpreted as the better coverage of the linker on the ZnO surface. Fig. 4(b) represents the image of the No–O_2 ZnO surface binding to DSP and Fig. 4(c) displays APTES molecule binding to ZnO on With-O_2 thin films. The fluorescence intensity was quantified based on a percentage, using eqn (2),

$$\%\ \text{Fluorescent pixels} = \left(\frac{\text{Fl}_o}{\text{Fl}_{total}}\right) \times 100 \qquad (2)$$

DSP shows approximately three times more binding on the ZnO surface than the APTES linker. This reiterates the utility of the zinc–thiol binding chemistry. Quantitative comparison of the two images confirms better fluorescent coverage in the case of a DSP linker.

3.3 Theoretical circuit analysis

The equivalent circuit representation of the ZnO biosensor was accomplished through a specific arrangement of the system's passive elements and their interactions with each other. The insets of Fig. 5(a) and (b) show the equivalent circuit model representation of the system for DSP and APTES linkers respectively. The resistance offered to the current flow due to molecular assembly is R_{ct}. The resistance offered by bulk ionic components in the buffer solution is R_s while R_{ZnO} denotes the resistance of the ZnO film. The contribution of double layer capacitance at the solution–electrode interface is C_{dl}. In the case of the DSP linker, C_{dl} is referred to as C_{DSP}. Note that C_{DSP} is the capacitance of the double layer formed by the binding of biomolecules to the DSP linker. On similar lines, in the case of APTES molecules, C_{dl} is referred to as C_{APTES} which is the double layer capacitance formed from the binding of biomolecules to APTES. C_{ZnO} is the inherent capacitance of ZnO resulting from its wurtzite crystal structure and polar surfaces.

The equivalent circuit diagrams for DSP and APTES linker functionalized sensor systems are shown in Fig. 5(a) and (b) respectively. The Zn–thiol interaction based sensor is imagined to be consisting of inner layer and outer layer, where the inner layer is formed due to the binding of thiol in DSP to individual zinc terminations and the outer layer is formed due to the binding of biomolecules. The APTES–oxygen interaction based sensor is imagined to be consisting of only one RC component, assuming that APTES will form a continuous monolayer on the surface, establishing a connected platform for antibody–antigen interactions. These equivalent circuit models were further analyzed using the Zview software (Scribner Associates Inc. – Southern Pines, NC). A comparison of simulated and experimental data using the DSP and APTES linkers for the 10 fg mL^{-1} and 1 ng mL^{-1} troponin-T concentrations is shown in Fig. 5(a) and (b) respectively. All simulations were performed using a constant phase element (CPE) instead of simple capacitance as it reflects non-homogeneity of the layer and is considered more appropriate for modelling of primary protein layers on the electrode surface.[4,22] The impedance values obtained experimentally were compared with the values obtained through model simulations using circuit diagrams. The difference between the simulated and experimental values was termed as an error and found to be less than 5%, which indicates relatively accurate fitting of the circuit model to the experimental data. EIS also allows for the identification of capacitance changes caused by the bio-recognition events at a metal oxide–liquid interface. These capacitance values were extracted for the 10 fg mL^{-1} and 1 ng mL^{-1} troponin-T concentrations by fitting the experimental data using the equivalent circuit diagrams. In the case of the DSP linker, the double layer capacitance varied from 1.1 μF to 1.8 μF over the range of 10 fg mL^{-1} to 1 ng mL^{-1} troponin-T concentrations as shown in the inset table in Fig. 5(a). Similarly, the inset table in Fig. 5(b) shows variation in double layer capacitance from 2.75 μF to 3 μF, when functionalized with an APTES linker. The data fitting to the equivalent circuit indicates the increase in capacitance of the double layer that is formed due to the antibody–antigen binding. The increasing capacitance values are hypothesized to be due to variation in dielectric permittivity as discussed earlier in the Results section.

When a system is perturbed due to addition of higher troponin-T concentration, it relaxes to a new steady state. The time taken for this relaxation is known as time constant $t = R_{ct}C_{dl}$. The analysis of this time constant gives an idea about the detection time. In the case of the DSP linker, the relaxation time was found to be 3.9 and 4.6 s respectively for 10 fg mL^{-1} and 1 ng mL^{-1} troponin-T concentrations. In the case of the APTES linker, it was found to be at 1.1 s for both 10 fg mL^{-1} and 1 ng mL^{-1} concentrations. Hence, it can be hypothesized that the detection time for lower and higher concentrations does not vary substantially.

These simulations were performed to understand the changes in the dynamic range of capacitance values due to the use of different linker chemistries. It can be observed that the dynamic range in terms of capacitance is wider for the DSP linker than that for the APTES linker.

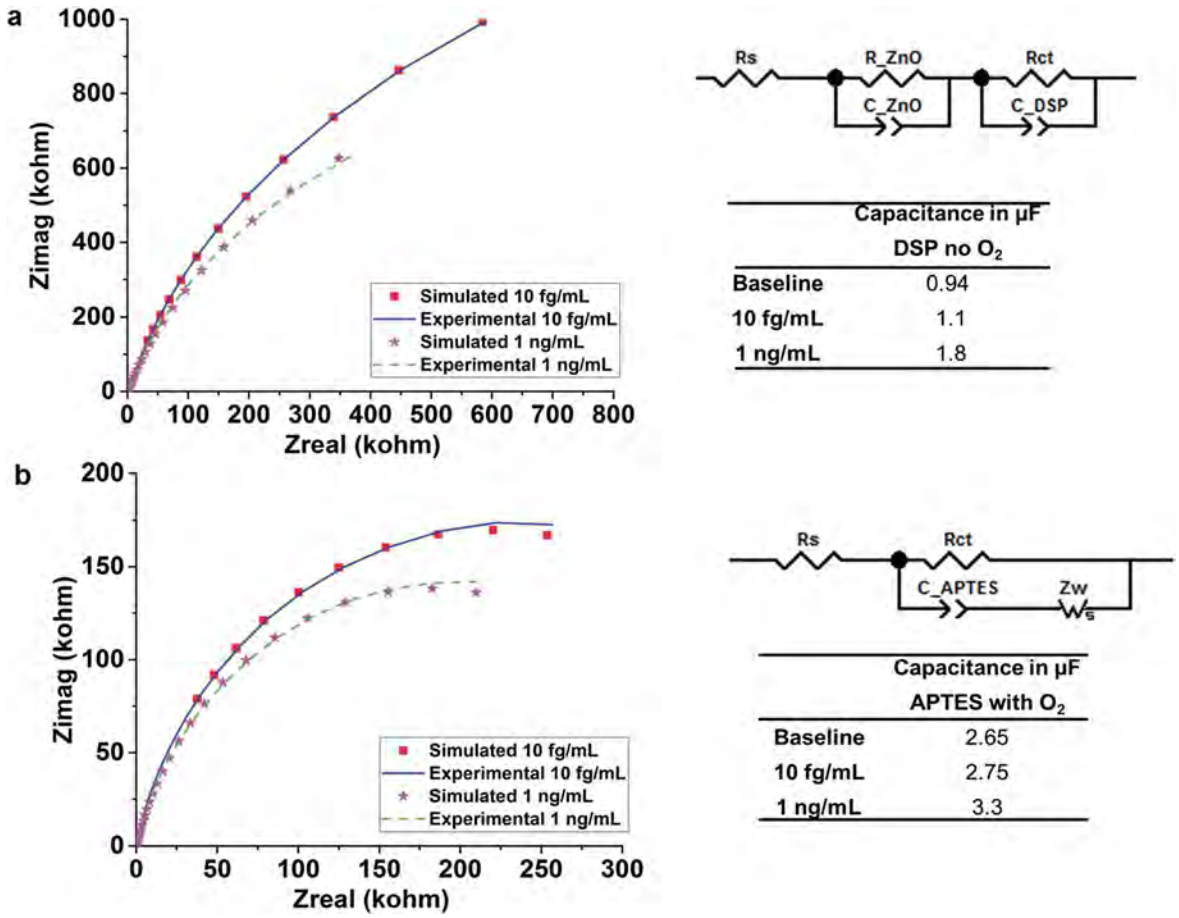

Fig. 5 (a) Simulated and experimental Nyquist plots using a DSP linker for 10 fg mL^{-1} and 1 ng mL^{-1} troponin-T concentrations diluted in PBS along with equivalent circuit diagram and extracted capacitance values; and (b) simulated and experimental Nyquist plots using an APTES linker for 10 fg mL^{-1} and 1 ng mL^{-1} troponin-T concentrations diluted in PBS along with equivalent circuit diagram and extracted capacitance values.

4. Conclusions

Numerous studies have been done to build biomonitoring diagnostic devices that will enable AMI patients to track their own condition, empowering them to take responsibility for their own health. The aim of this study is to demonstrate the potential utility of ZnO based affinity biosensors for point-of-care diagnostics. In this study, we investigated the role of zinc and oxygen surface terminations by utilizing two types of surface chemistries to design an ultra-sensitive ZnO based biosensor for troponin-T detection in human serum. The sensor performance was measured using non-faradaic electrochemical impedance measurements. Utilization of both DSP and APTES linkers resulted in the development of a biosensor that demonstrated linear dynamic range calibration for troponin-T within the clinically relevant concentration of troponin-T from ~10 pg mL^{-1} to 300 pg mL^{-1} in human serum. However, the enhanced performance of the sensor was achieved through leveraging the zinc–thiol interactions using DSP towards designing a robust immunoassay with the limit of detection as low as 10 fg mL^{-1}. EIS studies based on capturing the response of modulation of an electrical double layer proved effective in quantifying the relative affinities of different linkers and evaluating the ability of each linker to exploit the ZnO surface terminations. Fluorescence studies were also useful in gaining the confirmation of binding of two linkers on the ZnO surface. This study has contributed towards identifying successful functionalization of a ZnO semiconductor surface for building a bio-immunoassay, leading to ultra-sensitive detection of antigens. Hence, the results of this study are also very useful from the point of view of designing non-faradaic electronic detection systems using ZnO. Compared to current analysis techniques, this sensor demonstrates increased sensitivity as well as lowered complexity related to optical based detection. This work has demonstrated the potential for developing ultra-sensitive, novel diagnostic biosensors for rapidly detecting protein biomarkers for clinical point-of-care diagnostics. Future work includes testing this technology for multiplexed detection in order to build versatile POC devices.

Acknowledgements

We acknowledge the contribution of Dr Anjan Panneer Selvam for discussion and Mr Andi Wangzhou, Mr Shaji Chaudhry and Ms Sruti Bopanna from Biomedical Microdevices and Nanotechnology Laboratory at University of Texas at Dallas for

assisting in performing the experiments. We acknowledge the contribution of Mr. Vignesh Ravindranath for the design of front cover image. Funding for this project was supported by the Cecil H. and Ida Green endowed fellowship at University of Texas at Dallas.

Notes and references

1 H. Ay, E. M. Arsava and O. Sarıbaş, *Stroke*, 2002, **33**, 286–289.
2 H. A. Katus, A. Remppis, F. J. Neumann, T. Scheffold, K. W. Diederich, G. Vinar, A. Noe, G. Matern and W. Kuebler, *Circulation*, 1991, **83**, 902–912.
3 H.-S. Song, J.-H. Back, D.-K. Jin, P.-W. Chung, H.-S. Moon, B.-C. Suh, Y.-B. Kim, B. M. Kim, H. Y. Woo and Y. T. Lee, *Journal of Clinical Neurology*, 2008, **4**, 75–83.
4 E. P. Randviir and C. E. Banks, *Anal. Methods*, 2013, **5**, 1098–1115.
5 S. Gomes-Filho, A. Dias, M. Silva, B. Silva and R. Dutra, *Microchem. J.*, 2013, **109**, 10–15.
6 B. V. Silva, I. T. Cavalcanti, A. B. Mattos, P. Moura, T. S. Maria Del Pilar and R. F. Dutra, *Biosens. Bioelectron.*, 2010, **26**, 1062–1067.
7 F. T. Moreira, S. Sharma, R. A. Dutra, J. P. Noronha, A. E. Cass and M. G. F. Sales, *Sens. Actuators, B*, 2014, **196**, 123–132.
8 M. J. Spencer, *Prog. Mater. Sci.*, 2012, **57**, 437–486.
9 Y. Fu, J. Luo, X. Du, A. Flewitt, Y. Li, G. Markx, A. Walton and W. Milne, *Sens. Actuators, B*, 2010, **143**, 606–619.
10 X. Ren, D. Chen, X. Meng, F. Tang, X. Hou, D. Han and L. Zhang, *J. Colloid Interface Sci.*, 2009, **334**, 183–187.
11 S. Singh, S. K. Arya, P. Pandey, B. Malhotra, S. Saha, K. Sreenivas and V. Gupta, *Appl. Phys. Lett.*, 2007, **91**, 063901.
12 M. Willander, K. Khun and Z. H. Ibupoto, *Sensors*, 2014, **14**, 8605–8632.
13 V. A. Coleman and C. Jagadish, in *Zinc Oxide Bulk, Thin Films and Nanostructures*, ed. C. Jagadish and S. Pearton, Elsevier Science Ltd, Oxford, 2006, pp. 1–20, DOI: 10.1016/B978-008044722-3/50001-4.
14 Z. Fan and J. G. Lu, *J. Nanosci. Nanotechnol.*, 2005, **5**, 1561–1573.
15 C. Wöll, *Prog. Surf. Sci.*, 2007, **82**, 55–120.
16 P. W. Sadik, S. J. Pearton, D. P. Norton, E. Lambers and F. Ren, *J. Appl. Phys.*, 2007, **101**, 104514.
17 K. K. Jena, T. K. Rout, R. Narayan and K. V. Raju, *Polymer Int.*, 2012, **61**, 1101–1106.
18 A. Panneer Selvam and S. Prasad, *Future Cardiol.*, 2013, **9**, 137–147.
19 Z.-D. Gao, F.-F. Guan, C.-Y. Li, H.-F. Liu and Y.-Y. Song, *Biosens. Bioelectron.*, 2013, **41**, 771–775.
20 Y. Teng, X. Zhang, Y. Fu, H. Liu, Z. Wang, L. Jin and W. Zhang, *Biosens. Bioelectron.*, 2011, **26**, 4661–4666.
21 P. Tengvall, E. Jansson, A. Askendal, P. Thomsen and C. Gretzer, *Colloids Surf., B*, 2003, **28**, 261–272.
22 E. Katz and I. Willner, *Electroanalysis*, 2003, **15**, 913–947.
23 M. Bart, E. Stigter, H. Stapert, G. de Jong and W. van Bennekom, *Biosens. Bioelectron.*, 2005, **21**, 49–59.
24 D. A. Armbruster and T. Pry, *Clin. Biochem. Rev.*, 2008, **29**, S49–S52.
25 R. J. McEnroe, M. F. Burritt, D. M. Powers, D. W. Rheinheimer and B. H. Wallace, *Interference testing in clinical chemistry; approved guideline*, CLSI, Wayne, PA, 2nd edn, 2005.

A Novel Approach for Electrical Tuning of Nano-Textured Zinc Oxide Surfaces for Ultra-Sensitive Troponin-t Detection

Citation:

Munje, R. D., M. Jacobs, S. Muthukumar, B. Quadri, N. R. Shanmugam, et al. 2015. "A novel approach for electrical tuning of nano-textured zinc oxide surfaces for ultra-sensitive troponin-T detection." Analytical Methods 7(24): 10136-10144.